Predicting Summertime Caribbean Pressure in Early April

JOHN A. KNAFF*

Department of Atmospheric Science, Colorado State University, Fort Collins, Colorado

(Manuscript received 10 March 1997, in final form 25 March 1998)

ABSTRACT

A method to predict the June–September (JJAS) Caribbean sea level pressure anomalies (SLPAs) using data available the previous April is described. The method involves the creation of a multiple linear regression equation that uses three predictors. These predictors are the January–March (JFM) North Atlantic (50°–60°N, 10°–50°W) sea surface temperature anomalies (SSTAs), JFM Niño 3.4 (5°N–5°S, 120°–170°W) SSTAs, and the strength of the eastern Atlantic subtropical pressure ridge measured in March between 20° and 30°W. The physical role of each of the predictors in determining the variations of Caribbean SLPAs is discussed. The forecast equation is developed using a training dataset covering the period 1950–95 (46 yr) and is tested upon independent data covering the period 1903–49 where the data availability permits (42 yr). Results suggest that skillful forecasts are possible. The method reduced the interannual variance of the JJAS Caribbean SLPAs by 50% in the developmental dataset and by 40% in the independent dataset. Separate forecasts for the June–July and August–September SLPAs are also developed, tested, and discussed.

1. Introduction

Variations of summertime pressure in the Caribbean Sea have been long known to be related to Atlantic basin tropical cyclone (TC) activity and regional rainfall variations. Studies by Garriott (1906), Ray (1935), Brennan (1935), Namias (1955, 1969), Shapiro (1982a,b), Gray (1984), Gray et al. (1993, 1994), and Knaff (1997) have all shown the relationship between anomalously low Caribbean sea level pressure (SLP) and increased Atlantic TC activity. Shapiro (1982a,b) and Gray (1984) also indicate that predicting the summertime pressure can be accomplished by using the persistence of springtime (April–May) Caribbean and tropical Atlantic pressure. Gray (1984) utilized this springtime relationship as one component in his first forecast scheme of Atlantic TC activity. Not surprisingly, the same persistence-based forecast is still used in his revised early June forecast scheme (Gray et al. 1994).

The climatic impact of summertime Caribbean region pressure anomalies cannot be understated. An index of average June–September sea level pressure anomaly (SLPA) described in Gray (1984) containing the stations shown in Fig. 1 explains nearly 31% of the interannual variations of hurricanes and 29% of the year-to-year variations of intense (or major) hurricanes during the 1950–95 period. Pressure in the region has also been shown to be related to summer season rainfall (Hastenrath 1976). The Caribbean pressure variations are also associated with variations of the midlevel moisture fields and tropospheric vertical wind shears in the tropical Atlantic region (Knaff 1997). These summertime pressure variations, however, are very difficult to accurately predict, often changing abruptly prior to and during the Atlantic hurricane season (June–November). Until now, the average April–May pressure was the best known predictor of the upcoming summertime pressure. However, analysis shows April–May SLPAs explain only a small portion of the interannual variance of the same SLPAs during the months of June–September.

Other researchers have studied the relationship between Caribbean SLP and rainfall as they relate to the interannual variations of El Niño–Southern Oscillation (ENSO). These studies suggest that when the sea surface temperature (SST) conditions are anomalously warm in the eastern equatorial Pacific Ocean or when the Southern Oscillation index (normalized Tahiti minus Darwin SLPA) is negative, that warm season SLPAs tend to be higher than normal in the eastern tropical Atlantic and Caribbean Sea and lower than normal in the western Caribbean Sea and Gulf of Mexico (Wolter 1987; Hastenrath 1976, 1978; Covey and Hastenrath 1978). Along with these changes in pressure, warm season precipitation often decreases in the eastern Caribbean. Changes in the global orientation of the upper-level winds over the Tropics in association with ENSO

* Current affiliation: Cooperative Institute for Research in the Atmosphere, Colorado State University, Fort Collins, Colorado.

Corresponding author address: Dr. John A. Knaff, Department of Atmospheric Science, Colorado State University, Fort Collins, CO 80523.
E-mail: knaff@cira.colostate.edu

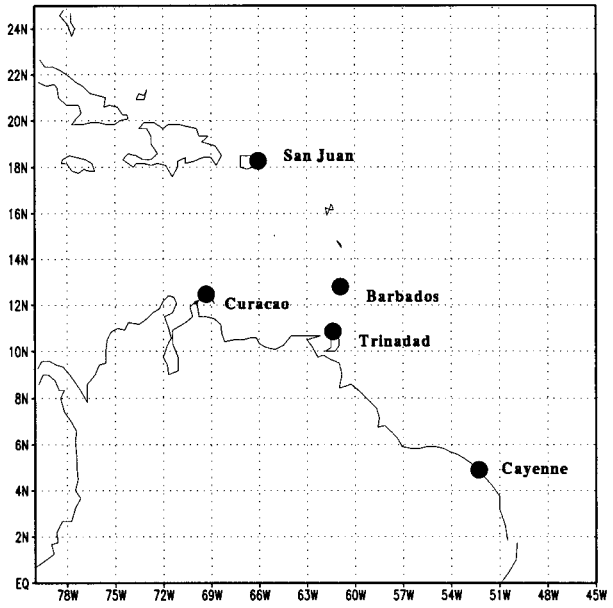

FIG. 1. Geographical locations of the stations used to create the Caribbean SLP indices.

variations have been shown to affect the location, frequency, and occurrence of tropical cyclones in the Atlantic basin (Goldenberg and Shapiro 1996; Gray 1984, 1988), which also impact the seasonal pressure field in this region (Knaff 1997).

In addition to the ENSO-related interannual variability of Caribbean SLPAs, studies have shown that the mean strength of the subtropical ridge in the Atlantic in the winter and spring seasons relate to the pressure anomalies that evolve in the Caribbean during the summer seasons (Namias 1972; Hastenrath 1978; Shapiro 1982a,b). This information, available well before the summer season begins, gives the motivation to examine the strength of the Atlantic subtropical ridge for the potential to predict summertime Caribbean SLPAs independent of the effects of ENSO. In this same spirit, it is thought that the multidecadal variation of the SSTs in the northernmost regions of the Atlantic Ocean (north of 45°N) are proxies for oceanic circulation changes, which act as the long-term pacemaker of the entire North Atlantic Ocean. These changes have been shown to be related to the midlatitude wind and pressure fields (Kushnir 1994; Peng and Fyfe 1996; Deser and Blackmon 1993; Kushnir and Held 1996). The multidecadal heating of the SSTs has been hypothesized to be related to changes in North Atlantic freshwater fluxes (Deser and Blackmon 1993), as well as more general variations in the strength of the Atlantic thermohaline circulation (Kushnir 1994).

The potential predictive relationships discussed above form the basis for the development of a forecasting scheme to predict summertime Caribbean SLPAs using data available prior to April. In section 2 the data and methodologies used in this study are discussed. Section 3 is a discussion of the statistical and spatial details of the above predictive relationships. The development of a regression-based forecast of summertime Caribbean SLPAs is discussed in section 4. These results lead to a unifying theory of how this portion of the climate system works, which is discussed in section 5, followed by brief summary in section 6.

2. Data and methodology

This study uses the pressure, wind, and SST fields from the Comprehensive Ocean Atmosphere Data Sets (COADS) as discussed in Shea et al. (1994). The SLP indices were calculated using data archived in the Global Historical Climatology Network (Vose et al. 1992) and updated by data obtained from Monthly Climatological Data of the World (U.S. Department of Commerce 1995a). The TC data used in this study is described in Neumann et al. (1993). Northern Hemisphere monthly mean 500-mb height fields (1950–94) described in Shea et al. (1994) are used for compositing studies.

Using COADS mean SLP, a mean Atlantic ridge between 20° and 30°W is created. This is accomplished by searching the grid data between the equator and 60°N for the highest value of pressure within the 20°–30°W longitude belt, which is the climatological location of the center of the Atlantic subtropical high during March. The six grid points found by the searching algorithm are then averaged to obtain the mean pressure and latitude of the ridge. These values from the COADS data are then extended through 1995 using data contained in the Climate Diagnostics Bulletins (U.S. Department of Commerce 1995b) and from values extracted from daily Atlantic surface analyses. This results in a continuous dataset for the 1950–95 period, which is used as the dependent or training period.

Multidecadal changes in the North Atlantic subtropical region are strongly related to changes that have occurred in the SST values in the region just south of the Arctic Circle. The North Atlantic (NATL) sea surface temperture anomalies (SSTAs) are created using average SSTs in the region from the reconstructed SST fields described in Smith et al. (1996). Anomalies are based on the 1950–79 mean. In addition, Niño 3.4 SSTAs were created using the same global datasets. An additional global SST climatology is used for independent testing of the forecast scheme for the time period 1903–49. These gridded data, developed at the Hadley Centre, were reconstructed in a similar manner as the Smith et al. data and are described in Parker et al. (1995).

Using the SLP data at the stations shown in Fig. 1, indices of Caribbean SLPA for the months of April–May (AM), June–September (JJAS), June–July (JJ), and August–September (AS) are created. These indices are created using the long-term means ($\overline{x_i}$) at each station (i) [see Eq. (1)]. An index (I_j) is found by summing the

TABLE 1. Yearly values of the Caribbean SLPA, March ridge, Niño 3.4 SSTAs, and NATL SSTAs. See text for explanation of the locations of the SSTA data. Listed from left to right are the March ridge strength, JFM Niño 3.4 SSTAs, JFM NATL SSTAs, AM Caribbean SLPA index, JJAS Caribbean SLPA index, JJ Caribbean SLPA index, and the AS Caribbean SLPA index.

Year	Mar ridge	Niño 3.4 SSTA	NATL SSTA	AM SLPA	JJAS SLPA	JJ SLPA	AS SLPA
1950	1022.92	−1.18	0.11	−0.30	−0.55	−0.30	−0.80
1951	1021.20	−0.50	0.03	−0.20	−0.70	−0.60	−0.80
1952	1017.47	0.26	0.15	−0.20	−0.20	0.00	−0.40
1953	1024.43	0.45	0.81	−0.30	−0.30	−0.20	−0.40
1954	1023.15	0.42	0.37	−0.10	−0.50	−0.80	−0.20
1955	1018.85	−0.78	0.61	−0.10	−0.95	−0.70	−1.20
1956	1023.37	−0.74	0.84	−0.20	0.10	0.20	0.00
1957	1019.65	0.09	0.29	0.40	−0.35	−0.40	−0.30
1958	1020.63	1.57	0.49	−1.20	−0.60	−0.40	−0.80
1959	1022.37	0.51	0.30	0.00	−0.10	0.10	−0.30
1960	1023.00	−0.02	0.10	−0.20	−0.20	−0.30	−0.10
1961	1020.62	−0.05	−0.10	0.70	0.25	0.30	0.20
1962	1019.58	−0.22	0.12	0.20	0.28	0.20	0.35
1963	1024.15	−0.27	0.36	−0.10	−0.30	−0.10	−0.50
1964	1019.83	0.45	0.57	0.30	−0.70	−0.90	−0.50
1965	1023.63	−0.24	0.51	−0.30	−0.12	0.20	−0.45
1966	1024.08	1.11	0.49	0.00	−0.40	−1.00	0.20
1967	1026.20	−0.29	0.39	0.30	−0.05	−0.50	0.40
1968	1026.02	−0.58	0.11	0.60	0.90	1.00	0.80
1969	1018.47	1.11	0.17	−1.20	−1.00	−0.80	−1.20
1970	1025.60	0.59	0.23	−0.20	−0.30	−0.10	−0.50
1971	1023.83	−1.20	0.13	0.20	0.35	0.50	0.20
1972	1024.38	−0.22	−0.29	0.00	0.10	0.00	0.20
1973	1023.12	1.27	−0.55	0.50	0.12	−0.20	0.45
1974	1024.30	−1.36	−0.62	1.20	0.30	0.40	0.20
1975	1023.70	−0.38	−0.61	0.40	0.50	0.50	0.50
1976	1023.58	−1.06	−0.31	0.70	0.88	1.00	0.75
1977	1023.73	0.60	−0.51	0.50	0.52	0.50	0.55
1978	1027.33	0.50	−0.05	−0.20	0.47	0.30	0.65
1979	1024.98	0.23	−0.05	0.00	0.00	0.40	−0.40
1980	1023.37	0.50	−0.18	0.10	0.25	0.30	0.20
1981	1020.97	−0.28	−0.05	−0.80	0.05	0.10	0.00
1982	1026.52	0.28	0.04	0.20	0.65	0.50	0.80
1983	1026.08	2.06	−0.35	−1.10	0.30	−0.50	1.10
1984	1021.40	0.00	−0.42	0.30	0.00	−0.30	0.30
1985	1024.55	−0.38	−0.42	0.30	0.30	0.60	0.00
1986	1028.38	−0.12	−0.56	−0.50	1.00	1.20	0.80
1987	1021.07	1.16	−0.53	−1.10	−0.28	−0.50	−0.05
1988	1024.70	0.61	−0.21	0.00	−0.20	0.10	−0.50
1989	1024.68	−1.15	−0.12	0.90	−0.25	0.60	−1.10
1990	1026.42	0.15	−0.63	−0.10	0.10	0.00	0.20
1991	1023.58	0.26	−0.66	0.50	0.88	0.40	1.35
1992	1029.82	1.80	−0.15	−1.10	0.43	0.40	0.45
1993	1019.00	0.29	−0.82	−0.90	0.48	0.10	0.85
1994	1028.50	−0.04	−0.84	0.80	1.12	1.00	1.25
1995	1024.00	0.89	−0.89	−0.20	−0.55	−0.60	−0.50

anomalies at each of the stations for each year (j) and dividing by the number of station used (N):

$$I_j = \sum_{i=1}^{N} \frac{x_i - \overline{x_i}}{N}. \quad (1)$$

Table 1 shows the resultant values of the ridge in millibars, the NATL SSTAs in degrees Celsius and Niño 3.4 SSTAs in degrees Celsius, and the indices of AM, JJAS, JJ, and AS Caribbean SLPAs in millibars. Detrending of these data is performed using simple linear regression (data vs time) in order to remove the strong multidecadal variations of the data in Table 1. This enables the examination of the interannual covariation more clearly. Note that for independent testing of this forecast scheme only one station Havana, Cuba (Casa Blanca), is used because it is the only station in the Caribbean region that has a long continuous record prior to 1950.

For this study, the January–March (JFM) SSTA in the Niño 3.4 region of the eastern equatorial Pacific is used, and is defined as the the area 5°N–5°S, 170°–120°W because of its relationship to ENSO core conditions and variations of Atlantic tropical cyclones (Barnston et al. 1997). The strength of the Atlantic subtropical ridge is represented by the mean strength of the March subtropical ridge in the Atlantic between 20° and

TABLE 2. Cross-correlation coefficients (×100) between the various predictors of interannual Caribbean sea level pressure variability and the predictands that represent the year-to-year fluctuations of SLP in this region. The diagonal position in this table gives the lag one autocorrelation coefficient (×100) of the quantity in that row/column. Statistical significance of these coefficients at the 10% level is indicated by bold print.

	Predictors				Predictands		
	NATL	Ridge	Niño 3.4	AM SLPA	JJAS	JJ	AS
NATL	81	−36	−7	−17	**−54**	**−40**	**−53**
Ridge	−36	15	7	5	**60**	**50**	**55**
Niño 3.4	−7	7	0	**−57**	−15	**−39**	10
AM SLPA	−17	5	**−57**	−1	**35**	**40**	**23**
JJAS	**−54**	**60**	−15	**35**	27	**85**	**89**
JJ	**−40**	**50**	**−39**	**40**	**85**	9	**52**
AS	**−53**	**55**	10	**23**	**89**	**52**	36

30°W and is referred to as ''the ridge'' from this point forward. The SSTA in the region, defined as the area 50°–60°N, 50°–10°W in the NATL, is chosen to represent the SST changes in this region. The yearly values of these SSTAs and SLPAs are listed in Table 1.

Using COADS, simple correlation and composite analyses are used to determine changes associated with the variations of the ridge, and NATL SSTAs and SLPAs listed in Table 1. Comparison of the predictions of summertime Caribbean pressure anomalies made by the AM persistence, the ridge, and the NATL SSTAs are then created. This will offer insight as to the cause of interannual summertime SLP variations.

Finally, empirical prediction schemes for the indices of Caribbean pressure are created using the method of leaps and bounds (Furnival et al. 1974). Potential predictors include the JFM NATL SSTAs, the JFM Niño 3.4 SSTAs, and the strength of the ridge during the month of March. The predictors were kept if, by their inclusion, they explained enough of the remaining variance of the predictand to be determined significant at the 10% level. More details of the model formulation and independent testing for the 1903–49 period will be discussed in section 4.

3. Results on dependent data

This section highlights results regarding the predictive skill of the ridge, Niño 3.4 SSTAs, and the NATL SSTAs as they relate to the summertime Caribbean SLPAs. These analyses contrast the current AM persistence-based forecast method to the ridge, ENSO, and NATL SSTA based forecasts and attempts to explain the relationship between these three predictors and summertime Caribbean pressure conditions through the analysis of monthly mean 500-mb height fields and COADS SSTs, winds, and pressures.

TABLE 3. Cross correlations (×100) between the linearly detrended potential predictors and the linearly detrended predictands.

	NATL	Ridge	Niño 3.4
JJAS	−30	44	−15
JJ	−28	35	−39
AS	−30	39	10

a. *Examination of relationships between the potential predictors*

One of the simplest ways of examining the relationships between the proposed predictors and summertime Caribbean SLPAs is to calculate cross-correlation and autocorrelation coefficients. Table 2 shows the cross correlations between both the predictors and predictands in the nondiagonal positions and the lag one autocorrelations of the various indices in the diagonal positions. The significance of the cross-correlation coefficients at the 10% level, calculated from a one-tailed Student's *t*-test, is indicated by bolder print. Note that the effects of strong autocorrelation are accounted for in the significance calculations. Large autocorrelations or serial correlations result in the reduction the number of degrees of freedom (*df*) (Barry and Perry 1973). To reduce the *df*, the method discussed in Leith (1973) is used. This method utilizes the integration of the serial correlations calculated at different lags to estimate the likely reduction in the *df*'s. In this case, lags were examined between −9 to +9 yr as suggested by Barry and Perry (1973, 235). This reduction is necessary for two of the predictors: the NATL SSTAs, where the number of degrees of freedom is reduced from 44 to roughly 10, and the ridge, where the *df* were reduced to 17. Throughout the rest of this paper, all significance calculations use this methodology. Table 3 shows the cross correlations obtained by linearly detrending both the potential predictors and the predictands for comparison.

The important feature in Table 2 is the good relationship between the proposed predictors and the summertime Caribbean SLPA indices. The weakest relationship is between the Niño 3.4 SSTA and the Caribbean pressures. The relationship is robust for the JJ period, but seems to switch its sign between the JJ to AS period. This is consistent with the results of Wolter (1987), who showed a similar sign reversal in cluster analysis from the winter months to late summer months. Also interesting to note is the relationship between the

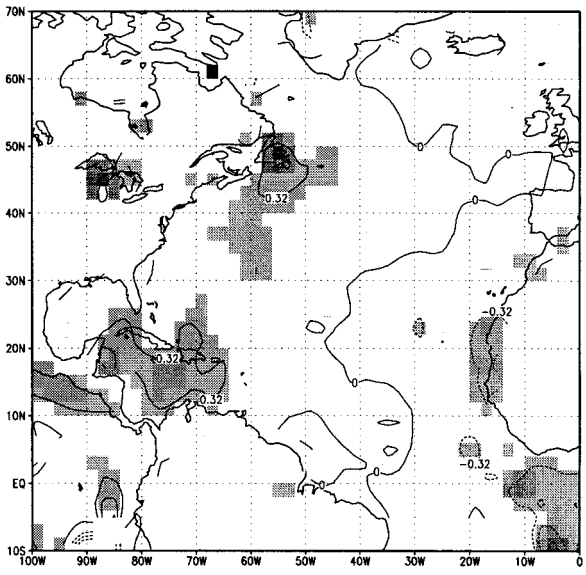

FIG. 2. Spatial characteristics of the correlation between the index of April–May Caribbean SLPs and COADS SLP during the following June–September periods. The contours are at the given increments of 10% of the variance explained or 0.55, 0.45, 0.32, 0.00, −0.32, −0.45, −0.55. Shading represents areas with significant correlations exceeding 10%.

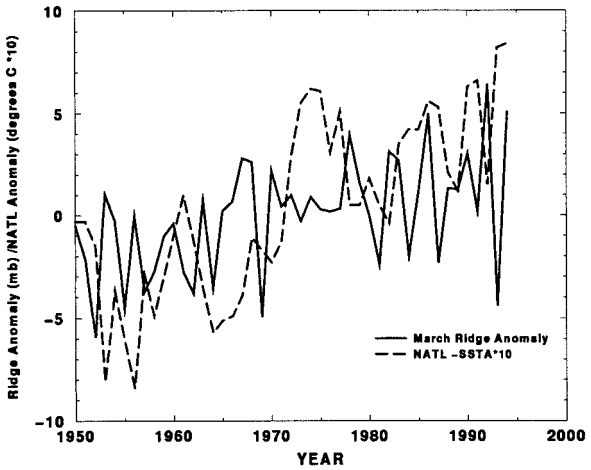

FIG. 3. Time series of the March ridge strength as measured by the pressure anomaly from the long-term mean in millibars along with the time series of the NATL SST anomalies. The NATL SST anomalies are multiplied by a factor of −10 for more easy comparison.

AM pressure index and the predictands. The utility of the AM pressure values for predicting summertime SLPAs becomes weaker as the lead time increases. This is likely the result of the strong relationship between the Niño 3.4 SSTA and the AM pressures coupled with both the observed tendency of ENSO-related indices to change sign during the spring (again see Wolter 1987 and Hastenrath 1976). Nonetheless, the AM pressure index explains a significant portion of the variance of SLP in the months to follow, as shown spatially in Fig. 2.

The NATL SSTAs are very slowly varying and are statistically (as well as physically) related to the strength of the Atlantic subtropical ridge. The multidecadal variation of the North Atlantic SSTAs and the east Atlantic subtropical ridge are fundamentally linked; when SSTAs in the North Atlantic are colder than normal, the pressures associated with the subtropical ridge are higher as shown in Fig. 3. This link, however, does not explain the large interannual variations that the ridge exhibits. It has long been known (Namias 1972; Hastenrath 1976; Shapiro 1982a,b) that variations of summertime SLPAs in the Caribbean are linked to variations in the strength of the subtropical high, which modulates the strength of the trade winds on an interannual basis. This link between the ridge and the SLPAs, though quite often mentioned in the literature, has seldom been exploited in a predictive sense. The combination of these two predictors captures the variations of two distinct timescales that occur in the NATL basin.

The spatial correlations between the ridge pressures and the NATL SSTAs and the JJAS pressures in the tropical North Atlantic region are shown in Figs. 4 and 5, respectively. Not surprisingly the spatial patterns shown in these two figures are similar, but the ridge explains a greater portion of the variance of the JJAS pressure field north of the Greater Antilles, while the NATL SSTA's significant results are primarily found in the Caribbean Sea region where decadal variations of tropical SSTs are prominent (Kushnir 1994).

Table 2 shows the weak relationship between the Niño 3.4 SSTAs and the other two potential predictors (the

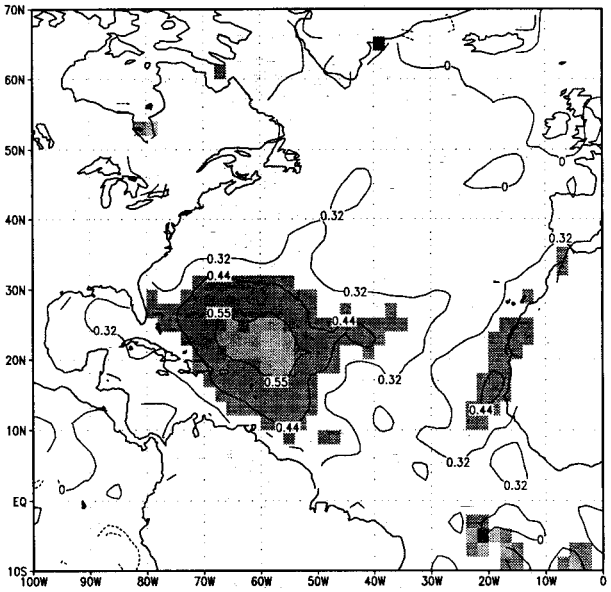

FIG. 4. Same as Fig. 2 except the correlation is between the strength of the Atlantic subtropical ridge between 20° and 30°W during the month of March and COADS SLP during the following June–September periods.

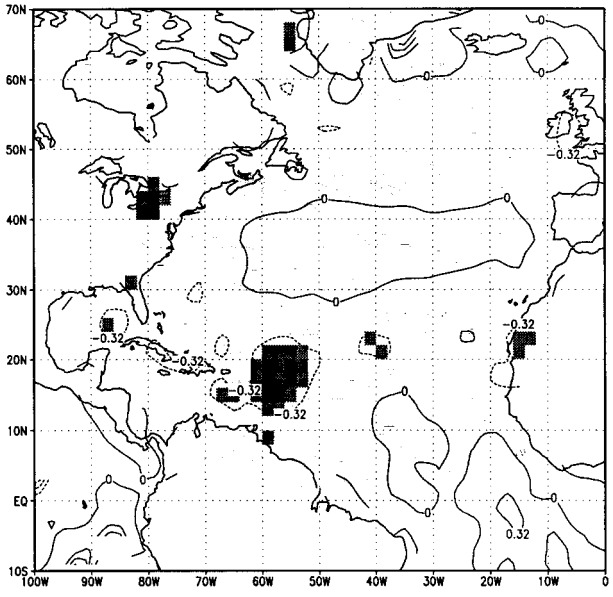

FIG. 5. Same as Fig. 2 except the correlation is between the NATL SSTAs during the months of January–March and COADS SLP during the following June–September periods.

NATL SSTAs and the ridge). This coupled with the decadal nature of the NATL SSTAs and the often independent interannual variations in the strength of the ridge gives confidence to the notion that the combination of these three predictors will create a skillful forecast of summertime Caribbean SLPAs.

From these analyses, it appears that the combination of the ridge, the NATL SSTAs, and JFM ENSO information will result in a drastic improvement in the ability to predict summertime SLP variations in the Caribbean Sea region. In addition, all of the information necessary to make such predictions is available in early April. A simple R^2 calculation using these parameters results in roughly a 50% reduction of the interannual variation of Caribbean SLPA compared to 12% using the traditional AM persistence-based relationship. With this information as motivation, the spatial aspects of these relationships will be further examined using compositing techniques.

b. Discussion of spatial composites

Figure 6 (top) shows February through March SLP composite differences between periods of cold conditions and periods of warm conditions in the NATL region, using 1953, 1954, 1955, 1956, 1958, 1959, 1964, 1965, 1966, and 1967 as the warm years and 1973, 1974, 1975, 1977, 1986, 1987, 1990, 1991, 1993, and 1994 as the cold years. Note the pressures in the vicinity of the subtropical high are on the order of 2 mb higher during the colder NATL period. In the lower half of Fig. 6 are the composite SST differences between periods of warm and cold conditions for the February

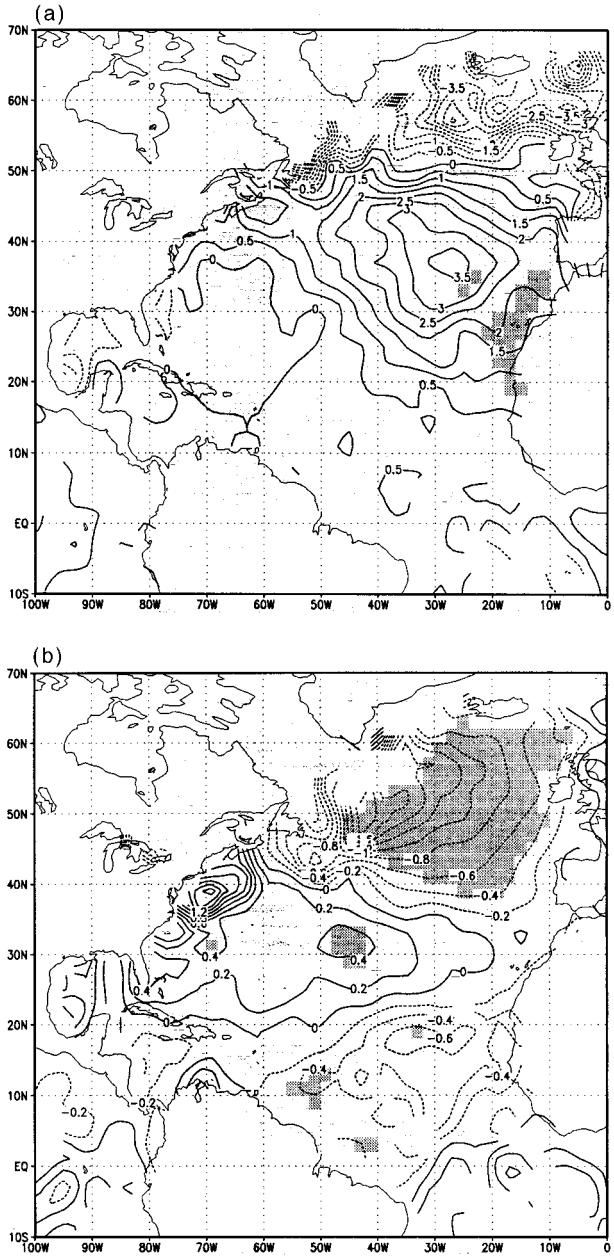

FIG. 6. February–March cold minus warm NATL SST composite differences of pressure (top) and of SST (bottom). Contours are of 0.5 mb and 0.2°C, respectively. The shading representing differences that are significant at at least the 10% level.

through March period. Clearly evident is the pattern of colder conditions north of 40°N, warm conditions in the subtropics, and cooler conditions again in the Tropics (see Fig. 5).

As the summer season is approached, the SST pattern shown in Fig. 6 (bottom) persists while changing little of its large-scale character. In the JJAS period (Fig. 7), pressures in the tropical Atlantic (top) are shown to react to the anomalous SST conditions (bottom) beneath them. It is the decadal SST change that seems to be the

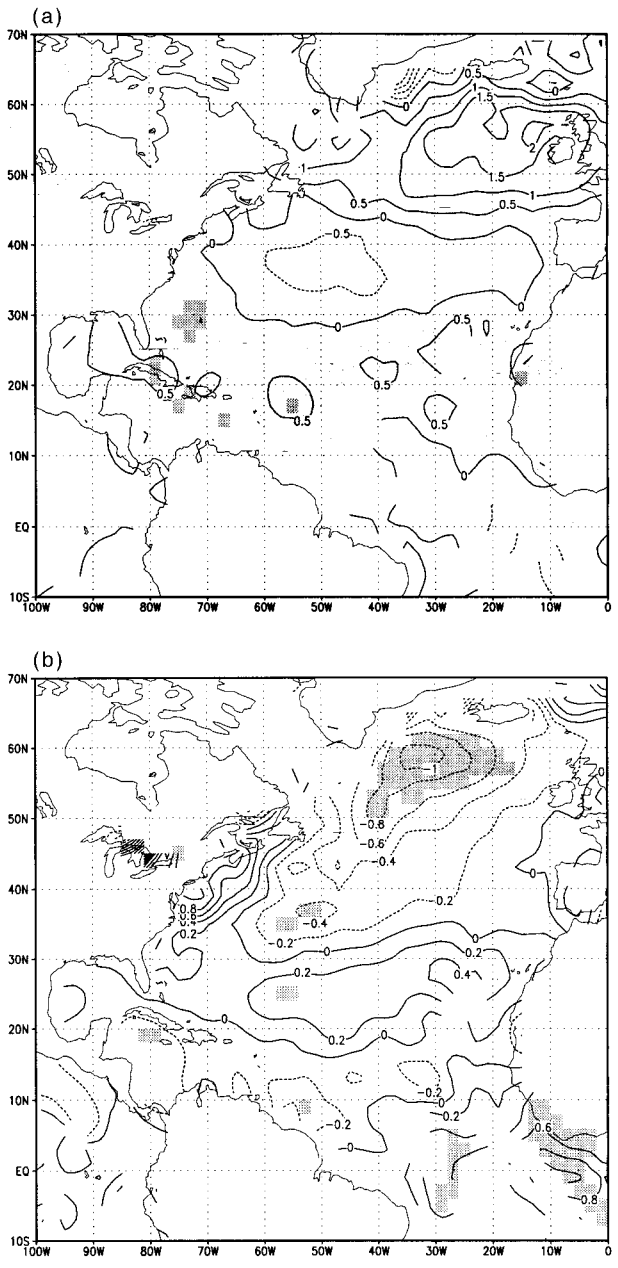

FIG. 7. Same as Fig. 6 except for the composite differences are for the June–September period.

driver of the predictive relationship between the NATL SSTAs and summertime SLPAs in the Caribbean region.

As mentioned previously, the ridge strength does not always follow the lead of the NATL SSTAs, but rather shows large interannual variations. This variation, clearly evident in Fig. 3, is thought to be caused by variations in midlatitude blocking. Examining the monthly mean Northern Hemisphere 500-mb height data during March, the preferred month for Atlantic atmospheric blocking events (see Rex 1950; Treidl et al. 1981), shows this to be the case. Figure 8 shows the strong (high pressure)

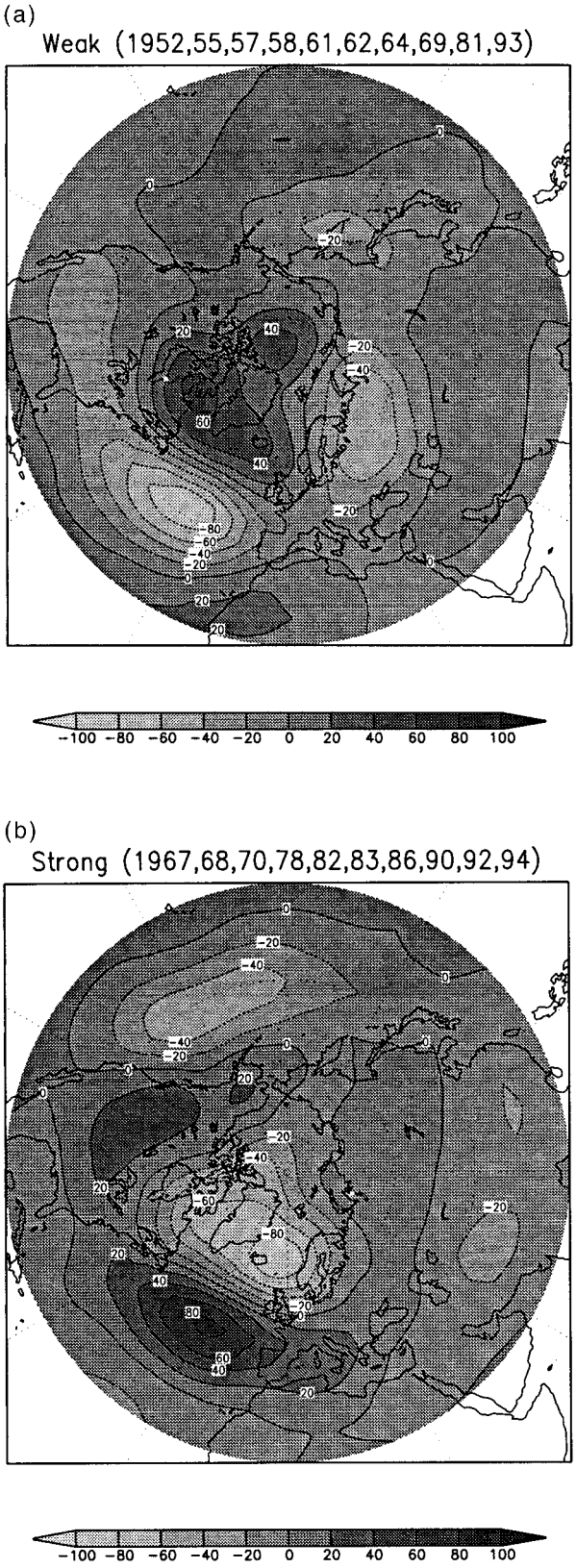

FIG. 8. March 500-mb height anomaly composites of the 10 weakest (top) and 10 strongest (bottom) ridge conditions. Anomalies are shown in m and dashed lines indicate negative anomalies.

ridge and weak (low pressure) ridge composite 500-mb height anomalies. In addition to results shown in Fig. 8, ridge-based composites are calculated differently in order to remove the strong decadal trends caused by, among other things, the variations of the NATL SST anomalies. Taking the the five strongest and five weakest ridge condition years in the multidecadal periods 1950–68 and 1969–94, the March 500-mb height conditions were composited. Figure 9 shows the composite of high minus low pressure ridge differences from these two multidecadal periods. These anomalies (Fig. 8) and differences (Fig. 9) indicate that when the ridge is strong there is little evidence of atmospheric blocking in the NATL. On the other hand, the weak ridge composite anomalies show clearly that zonal flow is occurring in the region normally occupied by the subtropical high, evidence of prolonged atmospheric blocking.

The COADS composites based on the strength of the ridge yield some rather interesting information. The years 1967, 1968, 1970, 1978, 1982, 1983, 1986, 1990, 1992, and 1994 are used for the strong (high pressure) ridge composite and 1952, 1955, 1957, 1958, 1961, 1962, 1964, 1969, 1981, and 1993 are used for the weak (low pressure) ridge composite. Interestingly, the JJAS SLP composites show significant differences throughout most of the tropical Atlantic, particularly in and around the Caribbean Sea (Fig. 10). These differences are larger and more statistically significant than those retrieved from the compositing of NATL conditions shown in Fig. 7. This suggests that in a sense the ridge-related atmospheric anomalies are superimposed upon the NATL SSTA-related changes of the JJAS tropical Atlantic SLP field.

As expected, these composites show significant differences in the strength of the subtropical ridge during the months of February and March. These ridge strength differences result in large (10%) differences in the strength of the North Atlantic trade winds as well as the strength of the northerly winds along the northwest coast of Africa. Even more interesting is the persistence of these wind conditions in the months continuing into summer. Table 4 shows the 2-month average values of ridge-based composite wind conditions and their differences of both the strength of the trade winds over a broad region of the tropical Atlantic as well as the northerly component of the wind just along and off the coast of Africa. The trades are weaker (stronger) during periods following weak (strong) ridge conditions.

Additional climate conditions found by the ridge-based composites are the tendency for cooler SSTs in the tropical regions of the Atlantic, and stronger sub-

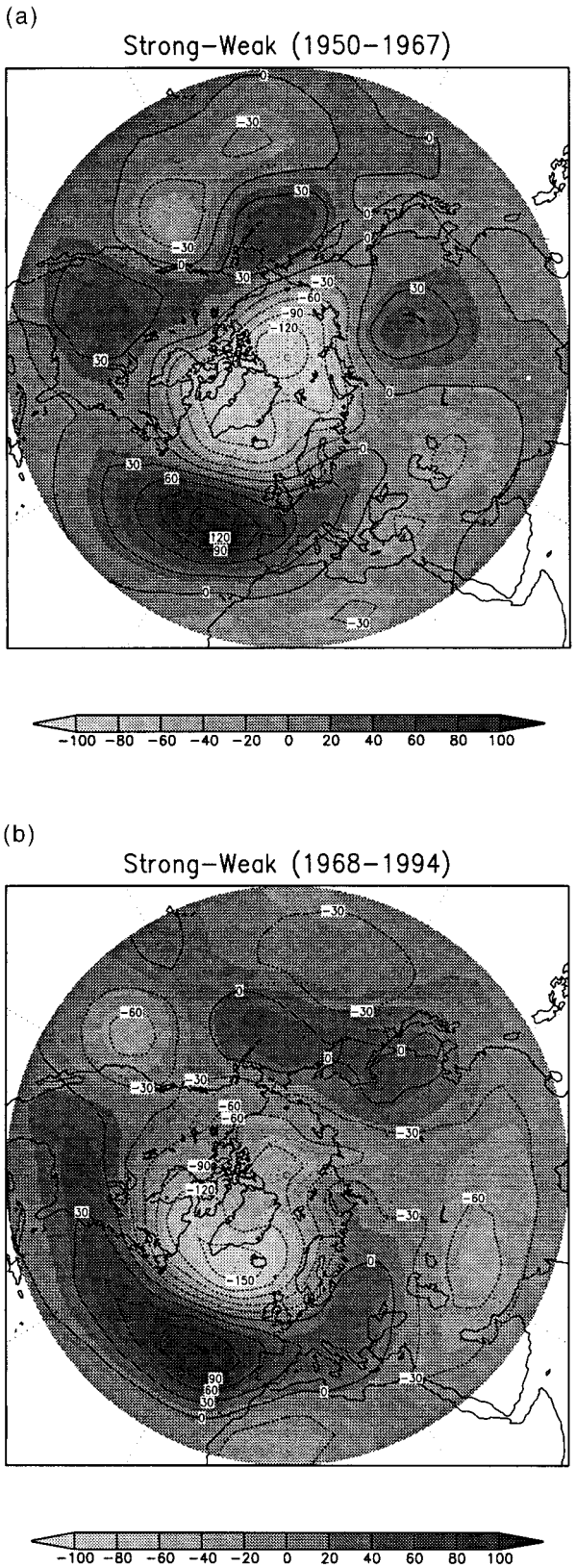

→

FIG. 9. March 500-mb height composite differences between the five strongest minus the five weakest ridge conditions during the period 1950–67 (top) and from 1968 to 1994 (bottom). Differences are shown as m and dashed lines indicate negative anomalies.

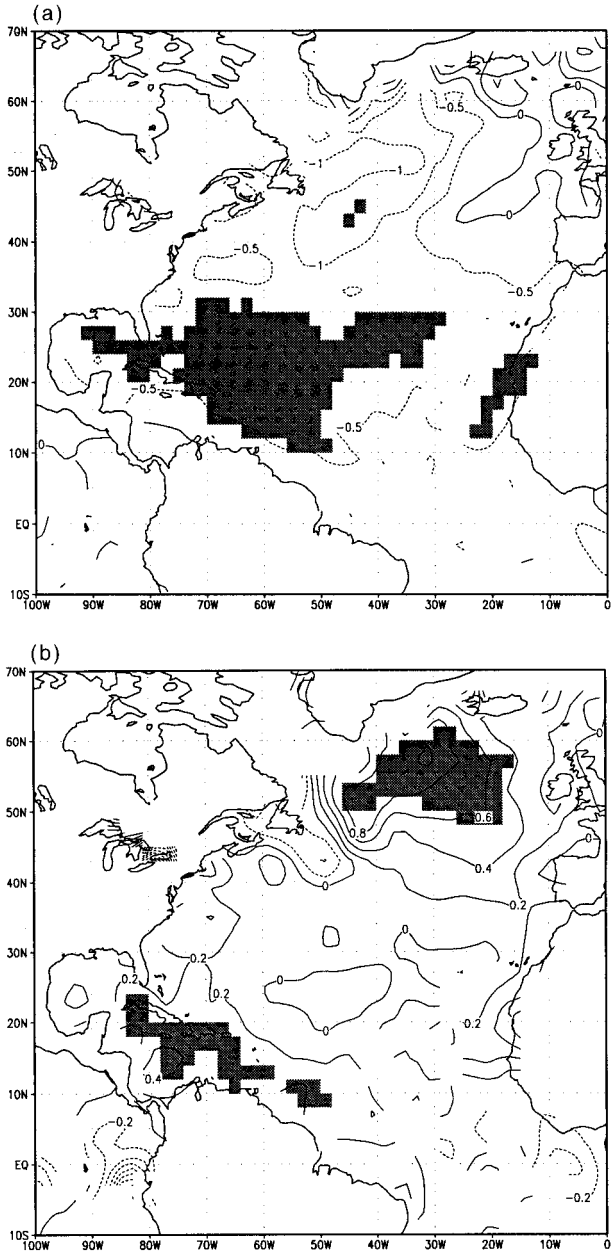

FIG. 10. June–September weak minus strong ridge composite differences of SLP (top) and of SST (bottom). Contours are of 0.5 mb and 0.2°C, respectively. The shading representing differences that are significant at at least the 10% level.

tropical ridge conditions during the summer period following strong ridge conditions in March. The stronger summertime subtropical high is thought to be the driver of the SST and pressure differences, but itself is the product of cooler subtropical SSTs caused by either the increase in wintertime westerly wind forced mixing (see Figs. 8 and 9) or by decadal variations related to the broad-scale North Atlantic SSTs. Using these relationships, a statistical model is constructed and tested in the section to follow.

TABLE 4. Magnitude of trade winds in the region 10°–20°N, 20°–80°W and the strength of northerly winds in the region 20°–30°N, 20°–30°W along the West African Coast composited by strength of the ridge. Composite averages and differences based upon the 10 weakest (low pressure) and 10 strongest (high pressure) ridge conditions are shown for 2-month periods along with the 6-month mean difference between the two quantities.

	Trade winds			Northerlies		
Months	Strong	Weak	Diff	Strong	Weak	Diff
Feb–Mar	6.68	6.06	0.62	−3.31	−2.19	−1.12
Apr–May	6.63	6.32	0.31	−4.00	−3.91	−0.09
Jun–Jul	7.14	6.47	0.67	−4.67	−4.40	−0.27
Aug–Sep	5.57	4.92	0.83	−4.16	−3.80	−0.46
Feb–Sep	6.55	5.94	0.61	−4.04	−3.58	−0.46

4. Forecast model formulation and testing

Using multiple linear regression and the method of leaps and bounds (Furnival and Wilson 1974), a forecast scheme to predict Caribbean SLP anomalies, which can be made in the first of April, is created. This scheme uses data from 1950 to 1995 as the training sample, and data from 1903 to 1949 as the verification data. The predictand is the JJAS Caribbean SLPA, and the predictors include the ridge strength (MR), the JFM Niño 3.4 SSTA (NINO), and the JFM NATL SSTA (NATL). These three predictors met the criteria discussed in section 2 and resulted in the explanation of 50% of the variance of the JJAS Caribbean SLPAs during the 46-yr training period. The resultant regression equation is shown below where $\beta_0 = -2.163$, $\beta_1 = 0.082$, $\beta_2 = -0.491$, and $\beta_3 = -0.127$:

$$\text{SLPA} = \beta_0 + \beta_1(\text{MR} - 1000\ \text{mb}) + \beta_2(\text{NATL}) + \beta_3(\text{NINO}). \quad (2)$$

From these coefficients the relationships between the predictors and the SLP can be inferred. Equation (2) implies that anomalously weak ridge conditions, warm NATL SSTs, and warm Niño 3.4 conditions would all result in lower than normal JJAS Caribbean SLP.

Surprisingly Niño 3.4 SST anomalies are negatively related to Caribbean SLPs. At first glance, this does not seem to make much sense, but examination of the June and July values of Caribbean SLPAs suggest that this affect is actually a result of the influence of central equatorial Pacific SSTs on early summer SLPs in the Caribbean. When the Niño 3.4 region is warmer than normal, pressures during the months of April through July in the Caribbean Sea region are lower than normal. In fact, the JJ SLPAs in the Caribbean area are fairly strongly negatively correlated ($r = -0.39$) with the JFM Niño 3.4 SSTAs (see Table 2). This relationship has the tendency to break down in the months of August and September. However, when forecasting the entire June through September period it is still important. When used in combination with ridge and NATL SST conditions, the Niño 3.4 SSTs explain an additional 4% of the variance. In this sense this term can be viewed as

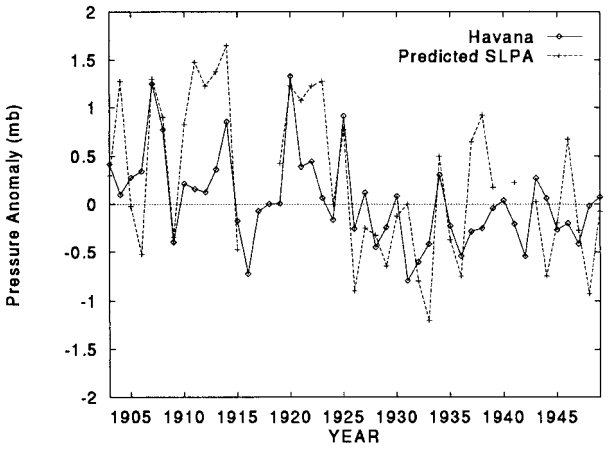

FIG. 11. Time series plot of the predicted JJAS Caribbean SLP anomaly and the JJAS Havana, Cuba, SLP anomaly for the period 1903–49. Note for years 1916–18, 1940, and 1942 forecasts are not made due to incomplete data. The anomaly correlation between the two series is $r = 0.63$, explaining 40% of the variance.

a correction term to the equation for years following cold or warm conditions in the eastern equatorial Pacific. However, the significance of this relationship still remains questionable, since it is barely acceptable under the criteria discussed in section 2.

To address the significance of the Niño 3.4 term as well as this method's significance in general, an independent forecast dataset is tested for the period 1903–49. This will best address the question of whether or not this scheme has skill when applied to forecasting Caribbean SLP anomalies. It also allows the better examination of the Niño 3.4 predictor and its overall impact on the scheme. For this test, the Parker et al.(1995) SST dataset (which starts in 1903) is used along with the pressure record of Havana, Cuba. The same methodology is used to calculate the March ridge conditions. However, the years 1916–18, 1940, and 1942 are not included in this test because of lack of adequate pressure information in the North Atlantic. This yields a 42-yr independent sample size for the tests.

The first question that must be addressed is whether or not this scheme has skill. Figure 11 shows the time series of the observed pressure anomaly at Havana along with the predicted value of the Caribbean SLPA for these periods. These time series compare quite well. In fact, the anomaly correlation between the two sets is $r = 0.63$, explaining 40% of the variance. This suggests that although some degradation occurred, this scheme has good skill.

A second test is performed to determine if the inclusion of Niño 3.4 information is useful in creating higher forecast skill. To this end, a model formulated with just the ridge and NATL SST information was created. The hindcast skill determined from the training period is equal to 46% reduction of the variance. When used to create independent forecasts, the skill dropped to 36% of the variance. Thus, the inclusion of the Niño 3.4 information retains the same skill improvement it had during the training period. For this reason JFM Niño 3.4 is kept as a predictor.

Keeping with the ideas of independent results, this regression equation was used to create a forecast of Caribbean SLP for the summer of 1996 using the values MR = 1018.8 mb, NATL = −0.10°C, and Niño = −0.74°C. The forecast scheme did quite well predicting a −0.47 mb pressure anomaly. The verification of this anomaly was −0.25 mb, but even more interesting were the details of how the pressure evolved. During the early months of summer, the pressure was extremely high, consistent with the occurrence of very cool SST conditions in the eastern equatorial Pacific. It was not until the third week of August that the pressures became extremely low. This was also about the time tropical cyclone development began to occur on a regular basis. The pressure remained extremely low, on the order of −1.0 mb during the period of September to early October, and thus the JJAS average was very close to the predicted value.

Using the same data, similar but slightly less skillful regression equations are created and tested for JJ and AS Caribbean SLP. As above, the coefficients for JJ are $\beta_0 = -1.878$, $\beta_1 = 0.083$, $\beta_2 = -0.374$, and $\beta_3 = -0.291$. The AS forecast uses only information from the ridge and the NATL SSTAs, and its coefficients are $\beta_0 = -1.907$, $\beta_1 = 0.082$, and $\beta_2 = -0.609$. Similar independent testing was performed on the JJ and AS regression equations, which explained 50% and 39% of the variance, respectively. Independent testing reveals that the JJ and AS regression equations explain 31% and 33% of the variance. The drastic degradation of the JJ equation is likely due to the midlatitude interference in the pressure field at Havana, and that the degradation would be much less if either more stations or if a station located farther south were used. The degradation of the AS forecast is what would be expected. These equations resulted in the JJ forecast of −0.07 mb (actual 0.9) and the AS forecast of −0.31 mb (actual −1.40) for the summer of 1996.

Similarly, forecasts were made for the summer of 1997, resulting in forecasts of −0.40 mb, −0.04 mb, and −0.19 mb, for JJAS, JJ, and AS, respectfully. Actual SLPAs for 1997 were 0.00 for JJ, −0.10 for AS, and 0.05 for the JJAS period. This year was characterized by weak ridge conditions (1021.1 mb), cold to neutral Niño 3.4 SSTAs (−0.31°C), and near-normal NATL SSTAs (0.02°C). The 1997 result is remarkable considering the strength of the ongoing warm ENSO conditions and the anomalously inactive Atlantic hurricane season.

5. Discussion

To a large degree the SSTAs in the tropical regions of the Atlantic during the summer months, particularly August and September, determine the SLP anomalies

that develop (see Knaff 1997, Fig. 13). These SSTs show distinct variability on a couple of distinct timescales. Easily seen in the time series of summertime Caribbean SLPAs and NATL SSTAs is the distinct decadal variability in which the SSTs were warmer than normal and SLPAs were lower than normal during the 1950s and 1960s (see Table 1). It is also clear that the decadal variability of summertime SLPAs in the Caribbean region is linked to the decadal variations of the NATL SSTAs. The other apparent timescale that the summertime pressures in the Caribbean operate on is interannual, manifested in the effects of ENSO, and of atmospheric blocking.

The effects of decadal variations of the SSTAs in the North Atlantic Ocean have been observed throughout the region. Among these, to list a few, are the long-running Sahel drought (Hastenrath 1990), the changes in the North Atlantic pressure oscillation (Hurrell 1995), and seasonal hurricane variations (Gray 1990) been hypothesized by Gray and Landsea (1993), Gray et al. (1996), and Kushnir (1994) that many of these changes are fundamentally related to the variations of the strength of the global oceanic thermohaline circulation. This circulation coined ''the conveyer belt'' (Broecker 1991) is driven by the buoyancy differences created by temperature and salinity of the waters of the North Atlantic. In this region, deep or bottom ocean water is formed by the sinking of cold and very saline water to great depths. It is hypothesized that when this circulation is running relatively fast, that warmer tropical water will be slowly taken farther north resulting in warmer basin-wide North Atlantic conditions. Likewise, a basin-wide cooling will result if this density-driven circulation slows.

It is proposed that much of the interannual variability of the SLP in the Caribbean is the result of the year-to-year variations of the circulation related to the Atlantic subtropical high or the ridge. Furthermore, it is suggested that a good measure of the strength of this circulation feature is available in the springtime strength of the subtropical ridge, which has been shown to be related to midlatitude blocking during the month of March—the height of Northern Hemisphere blocking activity.

Accepting the conclusion that the interannual variations of the March ridge are caused by variations of midlatitude blocking, the question of why would the ridge be related to JJAS Caribbean SLP must be answered. To answer this question, the results of the ridge-based composites discussed in section 3 are examined. Examining these composites in 2-month increments identifies two possible causes. The first is related to increased (decreased) wind stress along the West African coast when the ridge is strong (weak), as measured by the strength of the northerly component of the wind in this region (see Table 4). Increased wind stress in this area would result in increased oceanic upwelling of cooler water, eventually resulting in cooler SSTs in this region. These cooler waters could then have two affects on the surroundings. One affect would be through the advection of ocean water to the more tropical regions of the northeastern Atlantic, which would result in slightly higher pressures during the summer months. The other possible effect of increased upwelling would be the effect of increased evaporation by the trade winds downstream of the cooler upwelled water. The cooler underlying water would result in cooler and drier air parcels that would blow over the tropical Atlantic resulting in increased evaporative cooling of this region and higher pressures.

The other possible cause in these composites is the increase in the trade wind strength evident in Table 4. Increasing the magnitude of the trade winds would result in slightly more evaporation and cooling of the underlying ocean. This would again result in cooler SST conditions, which is consistent with higher summertime pressures. For instance, using the 6-month average difference of the trade wind strength, shown in Table 4, along with a bulk formula for latent heat, one can calculate the net affect of these wind differences:

$$\mathrm{LE} \approx L\rho_a U C_D q_s^*(1 - \mathrm{RH}). \qquad (3)$$

Using Eq. (3) with $U = 0.61$ m s^{-1}, RH = 85%, $q_s^* = 0.022$, $C_D = 0.7 \times 10^{-3}$, $\rho_a = 1.2$ kg m^{-3}, and $L = 2.5 \times 10^6$ J kg^{-1}, one can estimate the latent heat change associated with these wind differences. In this case the difference is approximately 4.2 W m^{-2}, which when applied over the 6-month period equates to approximately 6.5×10^7 J m^{-2}. Assuming the ocean mixed layer in the tropical Atlantic is 40 m deep, this energy difference amounts to a 0.39°C temperature change in that layer. This magnitude of temperature variation is often observed on interannual timescales.

One can carry this analysis one step further. If this temperature change is applied to the lowest 150 mb of the atmosphere, we can calculate a thickness change from which a change in SLP can be be calculated. This thickness change is on the order of a couple of meters resulting in approximately a 0.25-mb SLP change at the surface. This value is roughly what is observed in the ridge-based composite differences during the summer season (see the lower half of Fig. 10).

These considerations lead to the following hypothesis. The North Atlantic Ocean experiences dramatic decadal SST variability. Along with these long running periods of warmer (cooler) than normal SSTs, the tropical Atlantic, particularly in the lower Caribbean during the summertime, has shown similar decadal periods of lower (higher) surface pressure conditions. These conditions are physically linked and are the result of the atmosphere reacting hydrostatically to the temperatures of the surfaces below.

In addition to these long-running variations of pressures and SST in the North Atlantic, pressures also operate interannually as a response to variations of the strength of the northeastern Atlantic subtropical high or

ridge, a result of variations of springtime midlatitude blocking activity. During years with weak (strong) Atlantic subtropical ridge conditions during spring (March), trade winds and the northerly winds along the West African coast are weakened (strengthened). These wind differences act first in reducing (increasing) the rate of upwelling of cooler water along both the West African and northern South American coasts and second by reducing (increasing) the evaporation rate and latent heating over broad areas of the tropical Atlantic. These conditions result in a gradual warming (cooling) of SSTs in the tropical Atlantic region. The warm (cool) conditions that develop off the West African coast warm (cool) the lower atmosphere and reinforce the pressure anomaly and result in weak (strong) subtropical ridge conditions throughout the summer. This feedback results in the continuation of these anomalous wind conditions that act to further warm (cool) the tropical Atlantic. The resulting warm (cool) SST conditions that occur in the summer months affect the SLP field, ultimately resulting in anomalously low (high) SLP in the tropical Atlantic including the Caribbean Sea during the summer.

6. Summary

The previous sections have discussed the relationships between the east Atlantic subtropical ridge in March, JFM NATL SSTAs and the JFM conditions of the eastern equatorial Pacific, and the JJAS Caribbean SLPAs. Variations of the ridge and NATL SSTs are related to variations of pressure in the Caribbean regions in the following summer, affecting, among other things, the seasonal TC activity and rainfall in the Atlantic region. Furthermore, it is found that the combination of these factors in a multiple regression forecast scheme results in skillful prediction of Caribbean SLPAs. From this regression equation, it is shown that strong March ridge conditions, cool January through March NATL SSTs, and anomalously cold January through March Niño 3.4 conditions relate to higher than normal Caribbean SLP anomalies. The effects of the ridge and NATL SST are found to be the primary contributors to the prediction with the equatorial Pacific information acting as a correction term for early season (June–July) relationships between Caribbean pressure and Niño 3.4 SST anomalies. A hypothesis linking these relationships is presented. It is hoped that these studies will improve seasonal forecasting in the Caribbean region as well as improve understanding of tropical Atlantic climate variability.

Acknowledgments. The author wishes to thank Prof. William Gray, John Sheaffer, Chris Landsea, and Clara Deser for their discussions and comments regarding this research. I would also like to thank the Cooperative Institute for Research in the Atmosphere, Prof. Tom Vonder Haar, and Dr. Jim Purdom for allowing me the time to complete this task. Funding for this research was provided by NSF under Contracts ATM-9417563 (W. M. Gray, PI) with supplemental support given by the NASA Global Change Fellowship under Contract NGT-30147.

REFERENCES

Barnston, A., M. Chelliah, and S. Goldenberg, 1997: Documentation of a highly ENSO-related SST region in the equatorial Pacific. *Atmos.–Ocean,* **35,** 367–383.

Barry, R. G., and A. H. Perry, 1973: *Synoptic Climatology*. Harper and Row, 555 pp.

Brennan, J. F., 1935: Relation of May–June weather conditions in Jamaica to Caribbean tropical disturbances of the following season. *Mon. Wea. Rev.,* **63,** 13–14.

Broecker, W. S., 1991: The great ocean conveyor. *Oceanography,* **4,** 79–89.

Covey, D. L., and S. Hastenrath, 1978: Pacific El Niño phenomenon and the Atlantic circulation. *Mon. Wea. Rev.,* **106,** 1280–1287.

Deser, C., and M. Blackmon, 1993: Surface climate variations over the North Atlantic Ocean during winter: 1900–1989. *J. Climate,* **6,** 1743–1753.

Furnival, G. M., and R. W. Wilson Jr., 1974: Regression by leaps and bounds. *Technometrics,* **14,** 967–970.

Garriott, E. B., 1906: The West Indian hurricanes of September, 1906. *Mon. Wea. Rev.,* **33,** 416–423.

Goldenberg, S. B., and L. J. Shapiro, 1996: Physical mechanisms for the association of El Niño and West African rainfall with Atlantic major hurricane activity. *J. Climate,* **9,** 1169–1187.

Gray, W. M., 1984: Atlantic seasonal hurricane frequency. Part II: Forecasting its variability. *Mon. Wea. Rev.,* **112,** 1669–1683.

——, 1988: Environmental influences on tropical cyclones. *Aust. Meteor. Mag.,* **36,** 127–139.

——, 1990: Strong association between West African rainfall and U.S. landfall of intense hurricanes. *Science,* **249,** 1251–1256.

——, and C. W. Landsea, 1993: West African rainfall and Atlantic basin intense hurricane activity as proxy signals for the Atlantic conveyor belt circulation strength. Preprints, *Fourth Symp. on Global Change Studies,* Anaheim, CA, Amer. Meteor. Soc., 384–388.

——, ——, P. W. Mielke Jr., and K. J. Berry, 1993: Predicting Atlantic basin seasonal tropical storm activity by 1 August. *Wea. Forecasting,* **8,** 73–86.

——, ——, ——, and ——, 1994: Predicting Atlantic basin seasonal tropical storm activity by 1 June. *Wea. Forecasting,* **9,** 103–115.

——, J. D. Sheaffer, and C. W. Landsea, 1996: Climate trends associated with multi-decadal variability of intense Atlantic hurricane activity. *Hurricanes, Climatic Change and Socioeconomic Impacts: A Current Perspective,* H. F. Diaz and R. S. Pulwarty, Eds., Westview Press, 15–53.

Hastenrath, S., 1976: Variations in low-latitude circulation and extreme climatic events in the tropical Americas. *J. Atmos Sci.,* **33,** 202–215.

——, 1978: On modes of tropical circulation and climate anomalies. *J. Atmos. Sci.,* **35,** 2222–2231.

——, 1990: Decadal-scale changes of the circulation in the tropical Atlantic sector associated with the Sahel drought. *Int. J. Climatol.,* **10,** 459–472.

Hurrell J., 1995: Decadal trends in the North Atlantic oscillation and regional temperature and precipitation. *Science,* **269,** 676–679.

Knaff, J. A., 1997: Implications of summertime sea level pressure anomalies in the tropical Atlantic region. *J. Climate,* **10,** 789–804.

Kushnir, Y., 1994: Interdecadal variations in north Atlantic sea surface temperature and associated atmospheric conditions. *J. Climate,* **7,** 141–157.

——, and I. M. Held, 1996: Equilibrium atmospheric response to north Atlantic SST anomalies. *J. Climate,* **9,** 1208–1220.

Landsea, C. W., 1993: A climatology of intense (or major) Atlantic hurricanes. *Mon. Wea. Rev.,* **121,** 1703–1713.

Leith, C. E., 1973: The standard error of time-average estimates of climate means. *J. Appl. Meteor.,* **12,** 1066–1069.

Namias, J., 1955: Secular fluctuations in vulnerability to tropical cyclones in and of New England. *Mon. Wea. Rev.,* **83,** 155–162.

——, 1969: On the cause of the small number of Atlantic hurricanes in 1968. *Mon. Wea. Rev.,* **97,** 346–348.

——, 1972: Influence of Northern Hemisphere general circulation on drought in northeast Brazil. *Tellus,* **24,** 336–343.

Neumann, C. J., B. R. Jarvinen, A. C. Pike, and J. D. Elms, 1993: *Tropical Cyclones of the North Atlantic Ocean, 1871–1992.* National Climatic Data Center and National Hurricane Center, Coral Gables, FL, 193 pp. [Available from National Climatic Data Center, Asheville, NC 28801.]

Parker, D. E., M. Jackson, and E. B. Horton, 1995: The GISST2.2 sea surface temperature and sea-ice climatology. Climate Research Tech. Note 63, 48 pp. [Available from Hadley Centre for Climate Prediction and Research, Meteorology Office, London Road, Bracknell, Berkshire RG12 2SY, United Kingdom.]

Peng, S., and J. Fyfe, 1996: The coupled patterns between sea level pressure and sea surface temperature in the midlatitude north Atlantic. *J. Climate,* **9,** 1824–1839.

Ray, C. L., 1935: Relation of tropical cyclone frequency to summer pressure and ocean surface water temperatures. *Mon. Wea. Rev.,* **63,** 10–12.

Rex, D. F., 1950: Blocking action in the middle troposphere and its effects upon regions climate II: The climatology of blocking action. *Tellus,* **2,** 275–301.

Shapiro, L. J., 1982a: Hurricane climate fluctuations. Part I: Patterns and cycles. *Mon. Wea. Rev.,* **110,** 1007–1013.

——, 1982b: Hurricane climate fluctuations. Part II: Relation to large-scale circulation. *Mon. Wea. Rev.,* **110,** 1014–1023.

Shea, D. J., S. J. Worley, I. R. Stern, and T. J. Hoar, 1994: An introduction to atmospheric and oceanographic data. NCAR Tech. Note 404, 136 pp. [Available from National Center for Atmospheric Research, 1850 Table Mesa Drive, Boulder, CO 80307.]

Smith, T. M., R. W. Reynolds, R. E. Livezey, and D. C. Stokes, 1996: Reconstruction of historical sea surface temperatures using empirical orthogonal functions. *J. Climate,* **9,** 1403–1420.

Treidl, R. A., E. C. Birch, and P. Sajecki, 1981: Blocking action in the northern hemisphere: A climatological study. *Atmos.–Ocean,* **19,** 1–23.

U.S. Department of Commerce, 1995a: Monthly Climatic Data for the World. Vol. 48, No. 9, NOAA/NCDC/NESDIS. [Available from National Climatic Data Center, Asheville, NC 28801.]

——, 1995b: Climate Diagnostics Bulletin. No. 9, NOAA/NWC/NMC, 77 pp. [Available from Climate Prediction Center, W/NP52, Attn: Climate Diagnostic Bulletin, NOAA Science Center, Room 605, 5200 Auth Road, Washington, DC 20233.]

Vose, R. S., R. L. Schmoyer, P. M. Steurer, T. C. Peterson, R. Heim, T. R. Karl, and J. K. Eisheid, 1992: The Global Historical Climatology Network: Long-term monthly temperature, precipitation, sea level pressure, and station pressure data. Carbon Dioxide Information Analysis Center Publ. 3912, Oak Ridge National Laboratory, Environmental Science Division, U.S. Department of Energy, 189 pp. [Available from National Technical Information Service, 5285 Port Royal Rd. Springfield, VA 22161.]

Wolter, K., 1987: The Southern Oscillation in surface circulation and climate over the tropical Atlantic, eastern Pacific, and Indian Oceans as captured by cluster analysis. *J. Climate Appl. Meteor.,* **26,** 540–558.